Human Molecular Genetics, 2000, Vol. 9, No. 9 1303–1313

A novel protein with RNA-binding motifs interacts with ataxin-2

Hiroki Shibata, Duong P. Huynh and Stefan-M. Pulst*

Division of Neurology and Rose Moss Laboratory for Parkinson and Neurodegenerative Diseases, Burns and Allen Research Institute, Cedars-Sinai Medical Center, UCLA School of Medicine, Los Angeles, CA 90048, USA

Received 22 November 1999; Revised and Accepted 15 March 2000 DDBJ/EMBL/GenBank accession nos: human A2BP1, AF107103; P83A20, AL009266; T07D1.4, U41531; R74.5, Z36238; D2045.1, Z35639.

Spinocerebellar ataxia type 2 (SCA2) is caused by expansion of a polyglutamine tract in ataxin-2, a protein of unknown function. Using the yeast two-hybrid system, we identified a novel protein, A2BP1 (ataxin-2 binding protein 1) which binds to the C-terminus of ataxin-2. Northern blot analysis showed that A2BP1 was predominantly expressed in muscle and brain. By immunocfluorescent staining, A2BP1 and ataxin-2 were both localized to the *trans*-Golgi network. Immunocytochemistry showed that A2BP1 was expressed in the cytoplasm of Purkinje cells and dentate neurons in a pattern similar to that seen for ataxin-2 labeling. Western blot analysis of subcellular fractions indicated enrichment of A2BP1 in the same fractions as ataxin-2. Sequence analysis of the A2BP1 cDNA revealed an RNP motif that is highly conserved among RNA-binding proteins. A2BP1 had striking homology with a human cDNA clone, P83A20, of unknown function and at least two copies of A2BP1 homologs are found in the *Caenorhabditis elegans* genome database. A2BP1 and related proteins appear to form a novel gene family sharing RNA-binding motifs.

INTRODUCTION

Spinocerebellar ataxia type 2 (SCA2) is a member of the growing group of familial neurodegenerative diseases characterized by unstable CAG repeats which are expanded in patients. The causative genes for eight of these diseases, Huntington's disease (HD) (1), spinal and bulbar muscular atrophy (2), dentatorubral-pallidoluysian atrophy (DRPLA) (3,4), spinocerebellar ataxia type 1 (SCA1) (5), SCA2 (6–8), spinocerebellar ataxia type 3/Machado–Joseph disease (9), spinocerebellar ataxia type 6 (10) and spinocerebellar ataxia type 7 (11), have been identified and share no homology except for the CAG repeat encoding polyglutamine. Ubiquitinated intranuclear inclusions (NII) composed of aggregated proteins appear to be a common feature in the pathology of the triplet repeat diseases (12–20). The mechanism, however, by which the expansion triggers neuronal cell death has remained unclear. Recent studies have suggested that the formation of NII is not essential for the pathogenesis of HD or of SCA1 (21,22). This is further supported by the lack of NII in SCA2 patient brains (23).

Ataxin-2, the SCA2 gene product, is a highly basic protein (mol. wt 145 kDa) except for one acidic domain containing 50 acidic amino acids (amino acids 280–481), downstream of the poly(Q) tract (176–187). Within this domain, several putative functional motifs have been identified, such as a caspase-3 cleavage site (DXXD motif, amino acids 396–399) (24), RNA splicing motifs Sm1 and Sm2 (amino acids 284–341) (25), a clathrin-mediated *trans*-Golgi signal (YDS, amino acids 414–416) and an endoplasmic reticulum (ER) exit signal (ERD, amino acids 426–428) (26). The most common normal SCA2 alleles contain 22 or 23 CAG repeats with one or two CAA interruptions, whereas the repeat is expanded to >34 repeats without interruption in disease alleles (27). Despite the restricted pathology of SCA2 to the cerebellum and brainstem, the SCA2 transcript is widely expressed in various tissues, including heart, placenta, liver, skeletal muscle, pancreas and brain (6–8). Immunocytochemistry of normal and SCA2 brains showed that ataxin-2 expression was localized to the cytoplasm of specific neuronal groups, but was not restricted to Purkinje cells, which are the primary target of SCA2 pathogenesis (23). The level of ataxin-2 expression increased with age in neurologically normal brains and was greatly increased in abundance in brains from SCA2 patients (23).

Numerous novel and known proteins have been identified as specific binders of poly(Q) disease proteins. Proteins involved in vesicle trafficking (SH3GL3) (28), the cytoskeleton (HIP1) (29,30), protein degradation (HIP2) (31) and excitotoxic amino acid metabolism (CBS) (32), as well as proteins of unknown function (HAP1 and HYPs) (33,34), have been identified as binding proteins of the HD gene product, huntingtin. AIPs were identified as binding proteins of the DRPLA gene product, atrophin-1 (35). HYPs and AIPs share a WW domain in the critical binding region. Leucine-rich acidic nuclear protein (LANP), which is predominantly expressed in Purkinje cells, was identified as a binding protein of ataxin-1, the SCA1 gene product (36). The binding affinities did not always correlate with poly(Q) length. The affinities of HAP1, HYPA, HYPB and SH3GL3 for huntingtin binding and that of LANP for ataxin-1 binding were enhanced by poly(Q) expansion. The affinity of HIP1 for huntingtin binding was negatively modulated by the expansion. However, no obvious modulation by

*To whom correspondence should be addressed. Tel: +1 310 423 5166; Fax: +1 310 423 0149; Email: pulst@cshs.org

the length of the poly(Q) tract was observed in the binding affinities of HIP2 and of CBS for huntingtin and the affinity of AIPs for atrophin-1.

Here, we describe a novel ataxin-2 binding protein, designated ataxin-2 binding protein 1 (A2BP1), isolated by yeast two-hybrid screening. We show: (i) predominant expression of A2BP1 in brain and muscle; (ii) co-localization of A2BP1 and ataxin-2 in the *trans*-Golgi network; (iii) co-localization of A2BP1 and ataxin-2 in specific neurons; (iv) co-enrichment of both proteins in the same subcellular fractions. These data suggest that the specific binding of A2BP1 to ataxin-2 in brain may contribute to the restricted pathology of SCA2.

RESULTS

Identification of A2BP1

Using an ataxin-2 C-terminal fragment as bait, we isolated two positive clones in a yeast two-hybrid screen of 4.2×10^6 cells. Both clones encoded identical inserts of 1351 bp, including a poly(A) tail, predicting an open reading frame of 403 codons. This protein showed no match with the known protein sequences in the GenBank database and was designated A2BP1. By screening a brain cDNA phage library we identified an additional 16 clones. Nucleotide sequencing of the clones revealed multiple stop codons in the 5′-sequences immediately upstream of the sequence of the initial A2BP1 clone. Therefore, we concluded that the entire coding sequence (1131 bp, 377 amino acids) of A2BP1 was contained in the initial clone, pGAD10-A2BP1. Two in-frame deletions and one in-frame insertion were found in the additional A2BP1 clones. A 93 bp deletion was found in clone A2BP1-8 at positions 408–500. An 81 bp deletion was found in two clones (A2BP1-8 and A2BP1-13) at positions 617–697. A 54 bp insertion was found in clone A2BP1-14 at position 933. These deletions and insertions suggest alternative splicing of the A2BP1 transcript. From the deduced amino acid sequence of A2BP1, we found one RNP motif (amino acids 89–168) that is conserved among RNA-binding proteins such as hnRNPs, snRNPs, nucleolin and poly(A)-binding protein (37; Fig. 1). The characteristic feature of the motif is the presence of two highly conserved consensus sequences, RNP-1 (amino acids 136–142) and RNP-2 (amino acids 99–104). A BLAST search revealed that A2BP1 was a novel protein, but highly homologous to a human cDNA clone, P83A20, isolated from chromosome 22 (51.0% identity). Also, two *Caenorhabditis elegans* predicted genes, T07D1.4 and R74.5, were found to encode A2BP1 homologs (29.8 and 28.8% identity, respectively). In all four of these proteins, the consensus sequences, RNP-1 and RNP-2, were completely conserved except for the last amino acid of RNP-1 (Fig. 1).

Interaction of A2BP1 with ataxin-2 in yeast

We tested the binding of A2BP1 to ataxin-2 in the yeast two-hybrid system (Fig. 2A). The C-terminal fragment of ataxin-2 showed strong interaction with the full-length and C-terminal fragments of A2BP1. The full-length and the N-terminal fragments of ataxin-2 showed no interaction with any fragments of A2BP1. Thus, the essential domain for binding was localized to the C-terminal halves of ataxin-2 (amino acids 760–1312) and A2BP1 (amino acids 203–377). The RNP motif in A2BP1 or the acidic domain and the poly(Q) tract in ataxin-2 were not required for binding. We quantitated this binding ability as β-galactosidase activity by *o*-nitrophenylgalactoside (ONPG) liquid assay (Fig. 2B). Binding of the full-length A2BP1 fragment (56.2 ± 2.3 Miller units) to ataxin-2 was stronger than binding of the C-terminal fragment (19.4 ± 1.8 Miller units). This suggests that the N-terminus of A2BP1 is not essential for the binding but may enhance it.

Interaction of A2BP1 with ataxin-2 in human cells

We generated a rabbit polyclonal antiserum, 1734-2, against peptide A2BP1-B (amino acids 177–190 of human A2BP1). The specificity of the fifth bleed of antiserum was tested by western blot analysis (Fig. 3A). The antiserum detected four bands of 116, 66, 45 and 20 kDa. Since the preimmune serum detected 116, 66 and 20 kDa bands, these three bands appear to be non-specific and the 45 kDa band is the only one specific for 1734-2 antiserum. The epitope used for immunization is not conserved in the A2BP1 homolog P83A20. Therefore, we concluded that the band with a size of 45 kDa represents A2BP1. The size is slightly larger than the expected size of A2BP1 (40.6 kDa), probably due to post-translational modification.

To confirm the binding of A2BP1 to full-length ataxin-2 *in vivo* at physiological concentrations, we performed co-immunoprecipitation experiments of endogenously expressed ataxin-2 and A2BP1 from HTB10 neuroepithelioma cells. We used either ataxin-2 antiserum (1262-1) or A2BP-1 antiserum (1734-2) to precipitate the cell extract. Figure 3B shows a western blot of the precipitates detected by SCA2-B antibody. We observed a band of 145 kDa representing full-length ataxin-2 in samples precipitated with SCA2 (lane 2) and A2BP1 antisera (lane 4). The band was absent in lanes precipitated with preimmune sera (lanes 1 and 3). A second smaller band of 70 kDa was specifically observed in lanes 2 and 4. This 70 kDa band was previously observed using the SCA2-B antibody and represents a C-terminal ataxin-2 fragment (23).

Tissue specificity of A2BP1 transcripts

Northern blot analysis of human multiple tissues with a human A2BP1 *Eco*RI 0.7 kb fragment showed that A2BP1 was expressed in at least three isoforms of 6.2 (isoform 3), 4.4 (isoform 1) and 3.4 kb (isoform 2) (Fig. 4A). Among the three, isoform 1 (4.4 kb) was the major transcript observed in heart, whole brain and skeletal muscle (Fig. 4A, lanes 1, 2 and 6). Isoform 2 (3.4 kb) was also observed in these tissues, however, the expression in muscle (Fig. 4A, lanes 1 and 6) was significantly stronger than that in whole brain (Fig. 4A, lane 2). Isoform 3 (6.2 kb) was exclusively observed in whole brain (Fig. 4A, lane 2).

To study the expression of A2BP1 transcripts in brain tissues, northern blots of human multiple brain tissues were hybridized with the 0.7 kb A2BP1 probe. The same three isoforms were observed in all brain tissues tested except for spinal cord (Fig. 4C, lanes 1–3 and 5–8). The strongest expression of isoform 1 was observed in cerebellum (Fig. 4C, lane 1). Strong expression of isoforms 2 (3.4 kb) and 3 (6.2 kb) was observed in cerebral cortex, occipital pole, frontal lobe and putamen (Fig. 4C, lanes 2, 5, 6 and 8). Expression in medulla

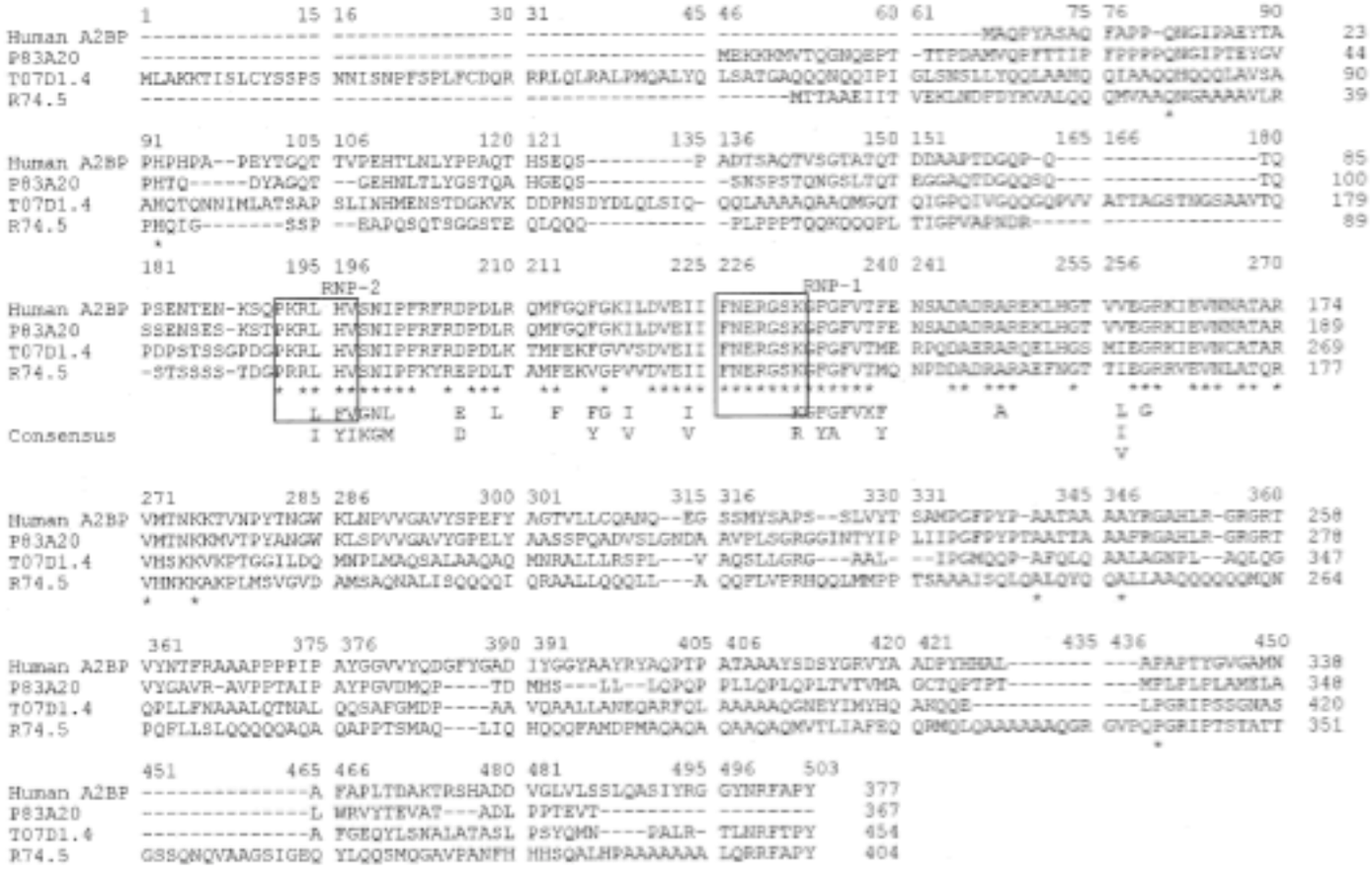

Figure 1. Alignment of the amino acid sequence of A2BP1 and related proteins. RNP-1 and RNP-2 are boxed. Asterisks represent amino acids conserved among all four proteins. The published consensus sequence for the entire RNP motif is shown at the bottom (37). Pairwise comparison reveals an overall level of 51.0% identity and 63.3% similarity between human A2BP1 and P823A20, 29.8% identity and 47.8% similarity between human A2BP1 and T07D1.4, 28.8% identity and 52.3% similarity between human A2BP1 and R74.1, 28.3% identity and 52.0% similarity between P83A20 and T07D1.4, 26.5% identity and 48.2% similarity between P83A20 and R74.1, 34.9% identity and 50.9% similarity between T07D1.4 and R74.1. All multiple and pairwise alignments were performed on the BCM Search Launcher site using ClustalW 1.7 (http://dot.imgen.bcm.tmc.edu:9331/multi-align/multi-align.html) and ALIGN (http://dot.imgen.bcm.tmc.edu:9331/seq-search/alignment.html), respectively.

was weak (Fig. 4C, lane 3) and not detectable in spinal cord (Fig. 4C, lane 3). The expression levels of all observed A2BP1 isoforms were lower than that of β-actin (Fig. 4D). An additional hybridization of the same blot with a longer *Bgl*II 1.4 kb fragment of A2BP1 showed an identical expression pattern (data not shown).

Biochemical analysis of A2BP1

For biochemical and immunohistochemical analyses of A2BP1, antiserum 1734-2 was further purified by affinity chromatography. On western blots of HTB10 protein extracts the A2BP1-B antibody detected a 45 kDa band which was slightly larger than the predicted size of A2BP1 (40.6 kDa) (Fig. 5A, lane 2). The p45 band is of identical size to the band previously detected with antiserum 1734-2 (Fig. 3A). Preimmune serum did not detect the p45 band (Fig. 5A, lane 1). In western blots of protein extracts from brain samples, the A2BP1-B antibody detected two major bands of 45 and 40 kDa (Fig. 5B, lanes 1 and 2, and C). In cerebellum samples, an additional band of 43 kDa was detected (Fig. 5C, lanes 2 and 4). A minor band of 29 kDa was observed in cerebral cortex and cerebellum (Fig. 5B, lane 2, and C). Peptide-absorbed A2BP1-B antibody failed to detect any of these bands (Fig. 5B, lanes 3 and 4). No significant differences in the number or intensity of detected bands were observed between extracts from normal and SCA2 brains (Fig. 5C).

Co-localization of A2BP1 and ataxin-2

In subcellular protein fractions of human brain tissues, A2BP1 was detected in the P3 endoplasmic reticulum (ER)/Golgi fraction and the S3 cytosolic fraction (Fig. 6B). The 145 kDa ataxin-2 band was also detected by SCA2-B antibody in the same fractions (Fig. 6A). No bands were detected in the nuclear (P1) and mitochondrial (P2) fractions (Fig. 6). The S3 fraction showed a stronger band intensity than P3 for both proteins. The purity of fractions was confirmed by analysis with an antibody to the *trans*-Golgi 58K protein (Fig. 6C) and an antibody to the neuronal nuclear protein NeuN (Fig. 6D). The levels of NeuN and *trans*-Golgi 58K were highly enriched in the nuclear fraction (P1) and the ER/Golgi fraction (P3), respectively, indicating that differential centrifugation had successfully separated these fractions.

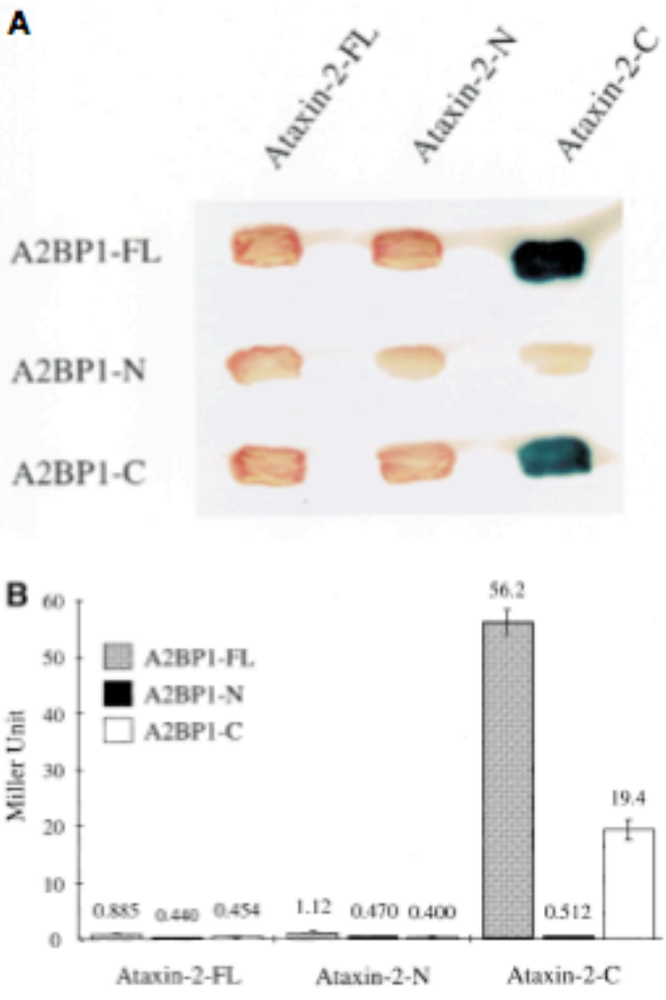

Figure 2. Yeast two-hybrid filter assay for interaction of ataxin-2 and A2BP1. (**A**) The SCA2 cDNA with CAG_{22} subcloned in pBDGAL4Cam and the A2BP1 cDNA subcloned in pGAD10 were co-transformed to test the interaction of ataxin-2 and A2BP1 in the yeast two-hybrid system. Ataxin-2 constructs contain amino acids 1–1312 (FL), 1–758 (N-terminal) and 760–1312 (C-terminal), respectively. Each fragment of A2BP1 contains amino acids 1–377 (FL), 1–203 (N-terminal) and 203–377 (C-terminal), respectively. On the filter incubated with X-gal, the blue color indicates the presence of β-galactosidase, indicating a positive test for interaction. (**B**) Results of the ONPG semi-quantitative assay. β-Galactosidase activity was calculated in triplicate and is shown in Miller units (38). Standard deviation is indicated by the vertical thin line on the top of each bar.

To further elucidate the co-localization of A2BP1 and ataxin-2, we co-stained COS1 monkey kidney cells using either the SCA2-A (Fig. 7a) or A2BP1-B antibody (Fig. 7e) and a mouse monoclonal antibody to γ-adaptin (Fig. 7b and f). The monoclonal anti-γ-adaptin antibody recognizes a 104 kDa polypeptide of the Golgi adaptor complex AP-1 which is localized primarily to the *trans*-Golgi network. Both the SCA2-A and A2BP1-B antibodies labeled the *trans*-Golgi organelles as recognized by the monoclonal anti-γ-adaptin antibody in COS1 cells (Fig. 7c and g). In addition, the A2BP1-B antibody (Fig. 7j) also co-labeled with GFP–ataxin-2(Q22) fusion protein (Fig. 7i) in COS1 cells.

To determine the relative distribution of the A2BP1 protein in human neurons expressing mutant ataxin-2 with an expanded poly(Q) tract, we co-labeled dentate neurons from an SCA2 individual with the A2BP1-B rabbit antibody (Fig. 7m) and the 1C2 mouse monoclonal antibody (Fig. 7n), which recognizes expanded poly(Q) repeats. A subset of cytoplasmic structures co-labeled with both antibodies. In general, more labeling was detected with the 1C2 antibody, so that some of the large cytoplasmic punctata were labeled exclusively by the 1C2 antibody.

Expression of A2BP1 in human tissues

To determine the cellular distribution of A2BP1 in human cerebellum, we stained sections from a neurologically normal individual with SCA2-B and A2BP1-B antibodies (Fig. 8). Preabsorption with peptide A2BP-B confirmed the specific immunoreactivity of the A2BP1 antibody (Fig. 8a and b). A2BP1 showed a punctate cytoplasmic staining in Purkinje cells (Fig. 8c) and in dentate neurons (Fig. 8d) which was similar to the distribution of ataxin-2 (Fig. 8g and h). Weak A2BP1 labeling was observed in small granule neurons and in glial cells (data not shown). The staining of both ataxin-2 and A2BP1 was punctate and distributed throughout the cytoplasm of Purkinje cells (Fig. 8c and g). In contrast, in dentate neurons A2BP1 as well as ataxin-2 were seen in a juxtanuclear location (Fig. 8d and h). To study co-localization in SCA2 cerebellum, we stained the brain of an SCA2 patient with A2BP1-B (Fig. 8e and f) and SCA2-B (Fig. 8i and j) antibodies. The staining intensity with both antibodies was significantly increased in the SCA2 cerebellum. Intranuclear aggregates or diffuse intranuclear staining were not seen with either antibody. An apparent increased intensity of A2BP1 labeling in SCA2 brains was seen in cerebella from two additional SCA2 patients and a normal control, one of which is shown in Figure 7.

DISCUSSION

A2BP1 binds to the ataxin-2 C-terminus

We identified a novel protein that binds to C-terminal domains of ataxin-2 (Fig. 2). Since the C-terminal ataxin-2 fragment does not include the poly(Q) tract, A2BP1 does not require the poly(Q) tract for binding. We tested the binding of A2BP1 to full-length ataxin-2 with expanded alleles containing 40 and 58 Q in the yeast two-hybrid system. The interaction of full-length ataxin-2 with A2BP1 was not recovered by the poly(Q) expansion (data not shown). The inability to detect the interaction of full-length ataxin-2 with A2BP1 in the yeast two-hybrid system is most likely due to steric hindrance, a low level of expression or the failure of nuclear localization of full-length ataxin-2 in yeast cells. In contrast, full-length ataxin-2 binds to A2BP1 in human cells at physiological concentrations, as shown by co-immunoprecipitation experiments (Fig. 3). In addition to full-length ataxin-2, a 70 kDa protein was also precipitated in these experiments. This protein is recognized by the SCA2-B antibody on western blots and represents a C-terminal fragment lacking the poly(Q) tract and the acidic domains (23). This further confirms that binding occurs via the C-terminal half of ataxin-2.

Tissue-specific expression of A2BP1 transcripts

Although the SCA2 transcript is ubiquitously expressed (6–8), SCA2 pathology is limited to specific neuronal populations. In contrast to this expression pattern, A2BP1 expression is more

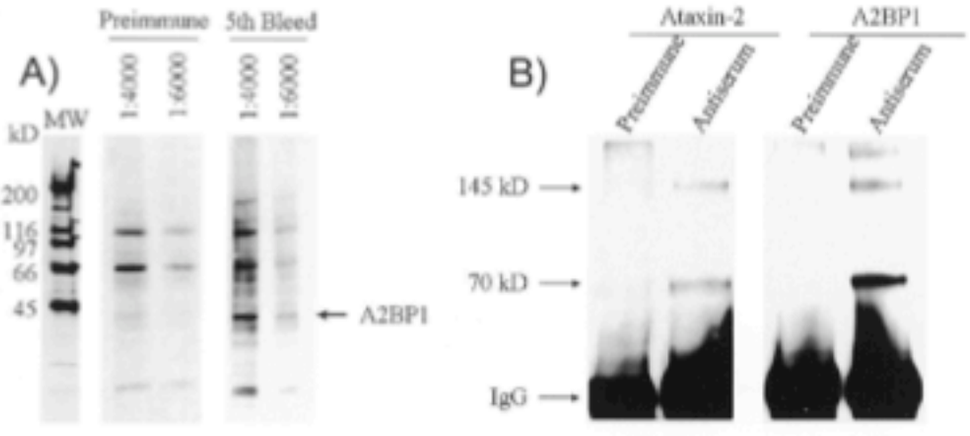

Figure 3. Co-immunoprecipitation of ataxin-2 and A2BP1. (**A**) Protein extracts from native HTB10 cells were blotted on membrane and detected by preimmune serum or the fifth bleed of antiserum 1734-2. Both sera were diluted at 1:4000 and 1:6000. The marker lane is shown on the right. The antiserum specifically recognizes A2BP1 with a relative molecular weight of 45 kDa. (**B**) Protein extracts from native HTB10 cells were immunoprecipitated with anti-ataxin-2 antiserum 1262-1 (lane 2) or anti-A2BP1 antiserum 1734-2 (lane 4) and detected on western blots using affinity-purified SCA2-B antibody. Lanes 1 and 3 show the results of precipitations with preimmune sera from 1262-1 and 1734-2 animals, respectively. Two specific bands of 145 and 70 kDa were observed in lanes 2 and 4. A common IgG band is also shown at the bottom of the picture.

restricted. Northern blot analysis showed three isoforms of A2BP1 in human brain (Fig. 4A and C). Isoform 1 (4.4 kb) was most commonly observed. The strongest expression of isoform 1 was observed in cerebellum (Fig. 4C, lane 1). The other two minor isoforms (3.4 and 6.2 kb) were predominantly observed in cerebral cortex, occipital pole, frontal lobe and putamen (Fig. 4C, lanes 2, 5, 6 and 8). This raises the possibility that binding to A2BP1 may be involved in the cell type-specific neuronal death seen in SCA2. Isoforms 1 (4.4 kb) and 2 (3.4 kb) were also observed in muscle tissues (Fig. 4A). A2BP1 expression has also been observed in heart as well as brain in mouse (H. Shibata and S.-M. Pulst, unpublished data). In this context it is interesting to note that patients with SCA2 often complain of muscle cramps, which may be related to ataxin-2 interaction with A2BP1.

Specificity of the A2BP1 antibody

Using the affinity-purified A2BP1-B antibody, we consistently detected a 45 kDa band, which is slightly larger than the calculated size of full-length A2BP1 (40.6 kDa) (Fig. 5). A 40 kDa isoform was also present in human brain samples. In addition, cerebellar extracts contained a 43 kDa band that was only seen in cerebellum (Fig. 5C, lanes 2 and 4). These proteins are very likely A2BP1 isoforms and not cross-reacting proteins, because preimmune sera or preabsorbed A2BP1 antibody failed to detect them. We also detected a minor band of 29 kDa which was enriched in the cerebellum (Fig. 5C).

A2BP1 is a member of a novel gene family sharing RNA-binding motifs

We found that A2BP1 has an RNP RNA-binding motif (amino acids 89–168). Ataxin-2 also contains two RNA splicing motifs, Sm1 and Sm2 (amino acids 284–341), which are shared with snRNPs (25). Interestingly, snRNPs have multiple RNP motifs which are present in A2BP1. Thus, the complex of ataxin-2 and A2BP1 may be involved in RNA processing. We identified one human (P83A20) and two *C.elegans* (T07D1.4 and R74.1) homologs of A2BP1 by database searching. The consensus sequences, RNP-1 and RNP-2, were common to all four proteins (Fig. 1). The RNP-1 motif, K-G-F-G-F-V-T-F/M, matched the consensus sequence K/R-G-F/Y-G/A-F-V-X-F/Y except for methionine at the last position of the two *C.elegans* proteins. In contrast, the RNP-2 motif, L-H-V-S-N-I, showed complete conservation among the four proteins. A single amino acid, the terminal I, diverged from the established consensus sequence, L/I-F/Y-V/I-G/K-N/G-L/M (37). In addition, the entire RNP region (amino acids 87–169 of human A2BP1) showed an extremely high conservation. Fifty-two out of 83 amino acids were identical in the four proteins. The level of conservation within other protein families with RNP motifs, such as hnRNPs, is significantly lower than that shown here. This strongly suggests that A2BP1 is a member of a novel gene family characterized by this highly conserved RNP motif. RNA-binding proteins with RNP motifs are involved in various RNA metabolic functions such as RNA processing and intracellular RNA transport (37). The evolutionary conservation suggests that proteins in this family may be involved in critical steps of RNA processing.

Expression of ataxin-2 and A2BP1 in human neurons

In all tested brain samples, ataxin-2 and A2BP1 showed almost identical staining patterns (Figs 7 and 8). Both proteins were abundantly expressed in the cytoplasm of Purkinje cells and dentate neurons. The staining in dentate neurons was intense and juxtanuclear. The staining in Purkinje neurons was less intense and more punctate. Large punctate structures were also observed in a juxtanuclear position, although they were less intense than in dentate neurons. This juxtanuclear localization of both proteins in both neuronal types is very similar to the pattern of the Golgi apparatus in COS1 cells shown in Figure 7. The presence of a clathrin-mediated *trans*-Golgi signal (amino acids 414–416), co-enrichment of both proteins in the ER/Golgi subcellular fraction and co-localization with γ-adaptin in the *trans*-Golgi network are consistent with this

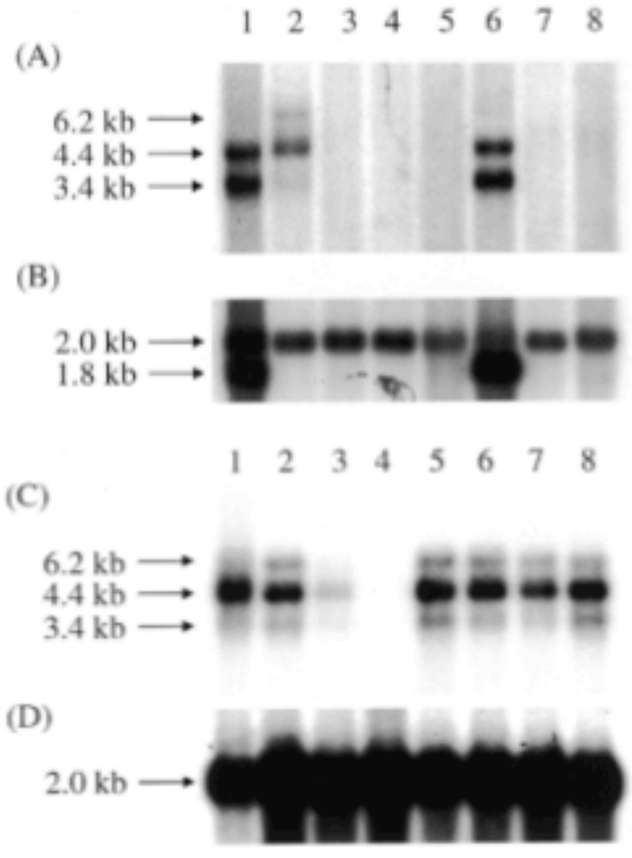

Figure 4. Northern blot analysis of A2BP1 expression. (**A**) Human multiple tissue northern blots were hybridized with the *Eco*RI 0.7 kb fragment of human A2BP1 as a probe. Each lane contains ~2 µg of poly(A)$^+$ RNA from the following human tissues: heart (lane 1), whole brain (lane 2), placenta (lane 3), lung (lane 4), liver (lane 5), skeletal muscle (lane 6), kidney (lane 7) and pancreas (lane 8). Arrows point to bands with approximate sizes 6.2, 4.4 and 3.4 kb. Two transcripts of 3.4 and 4.4 kb were observed in heart, whole brain and skeletal muscle (lanes 1, 2 and 6). The largest transcript (6.4 kb) was observed exclusively in whole brain. (**B**) Human multiple tissue northern blots were hybridized with a 1.8 kb β-actin probe (Clontech). The equal signal intensity of β-actin with a size of 2.0 kb shows near equal amounts of total RNA loaded in each lane. The α-actin band with a size of 1.8 kb was specifically observed in heart and skeletal muscle (lanes 1 and 6). (**C**) Northern blots of human brain RNAs hybridized with the same A2BP1 probe as in (A). Each lane contains ~2 µg of poly(A)$^+$ RNA from the following human brain tissues: cerebellum (lane 1), cerebral cortex (lane 2), medulla (lane 3), spinal cord (lane 4), occipital pole (lane 5), frontal lobe (lane 6), temporal lobe (lane 7) and putamen (lane 8). (**D**) Hybridization with a β-actin probe was as in (B).

observation (Fig. 6). In sections from three SCA2 brains neuronal labeling for A2BP1 as well as ataxin-2 appeared to be enhanced and was more diffusely distributed, suggesting that A2BP1 may be involved in SCA2 pathogenesis (Fig. 8). However, these observations need to be interpreted with caution due to inherent variability in tissue processing and fixation. Using the mouse monoclonal 1C2 antibody and the rabbit polyclonal A2BP1 antibody, it was possible to examine co-localization in brains of SCA2 patients (Fig. 7m and n). Ataxin-2 and A2BP1 were co-localized in a subset of cytoplasmic structures, although some cytoplasmic structures were only stained by the 1C2 antibody (Fig. 7p).

The physiological role of ataxin-2/A2BP1 interaction deserves further study. If the RNA-binding domains in both proteins are functional, one possible role of the ataxin-2–A2BP1 complex may be RNA transport in neurons. Neuronal cytotoxicity of ataxin-2 with expanded poly(Q) tracts might be due to altered RNA transport function. This hypothesis is consistent with the absence of intranuclear inclusions or aggregates in SCA2 (23) whereas these are commonly reported in other triplet repeat diseases (12–20).

MATERIALS AND METHODS

Identification of ataxin-2-binding proteins

A 3′ cDNA fragment corresponding to a C-terminal fragment (amino acids 817–1312) of ataxin-2 was amplified by PCR and subcloned into the pBDGal4Cam vector (Stratagene). Using the resulting plasmid, pBD-SCA2-U4L2, as bait, yeast two-hybrid screening of a human fetal brain cDNA library in construct pGAD10 was performed following the supplier's protocol (Clontech). Upon screening 4.2×10^6 colonies, two positive clones were identified. The plasmids were recovered from both yeast clones and used in *Escherichia coli* transformation. Both plasmids contained the identical insert by nucleotide sequencing. One plasmid, pGAD10-A2BP1, encoding the entire coding sequence of A2BP1, was digested with *Eco*RI to recover N-terminal (amino acids 1–203) and C-terminal (amino acids 203–377) fragments. The A2BP1 fragments were recloned in pGAD10 and used in co-transformation of a yeast host strain, Y190, with pBDGAL4Cam constructs encoding full-length, N-terminal and C-terminal ataxin-2 fragments fused to the GAL4-binding domain. The double transformants were selected on SC medium without leucine and tryptophan. The β-galactosidase filter assay was performed by incubating freeze-fractured colonies on Opti-tran membrane (Schleicher & Schuell) in Z-buffer (60 mM NaH_2PO_4, 40 mM Na_2HPO_4, 10 mM KCl, 1 mM $MgSO_4$, pH 7.0, 0.03 mM β-mercaptoethanol, 2.5 mM X-gal) at 37°C for 30–480 min. The semi-quantitative β-galactosidase assay was performed by monitoring hydrolysis of ONPG in Z-buffer as previously described (38).

cDNA screening

Additional cDNA sequence of A2BP1 was obtained by database searching and by screening of a gridded human cDNA library (Genome Systems, Palo Alto, CA). The procedures for library screening followed the suppliers' protocol (Genome Systems).

Northern blot analysis

A human multiple tissue Northern Blot (Clontech, Palo Alto, CA) and a human brain multiple tissue Northern Blot II (Clontech) were probed with an *Eco*RI 0.7 kb fragment of human A2BP1. The probes were labeled with [α-^{32}P]dCTP using a RadPrime random priming kit (Gibco BRL, Rockville, MD). The conditions of hybridization and washing followed the supplier's protocols (Clontech). The relative loading and integrity of total RNA on each lane were confirmed by subsequent hybridization with β-actin (Clontech).

Antibodies

Two rabbits were injected with two peptides of human ataxin-2 (peptide SCA2-A, amino acids 359–371, AKVNGE-

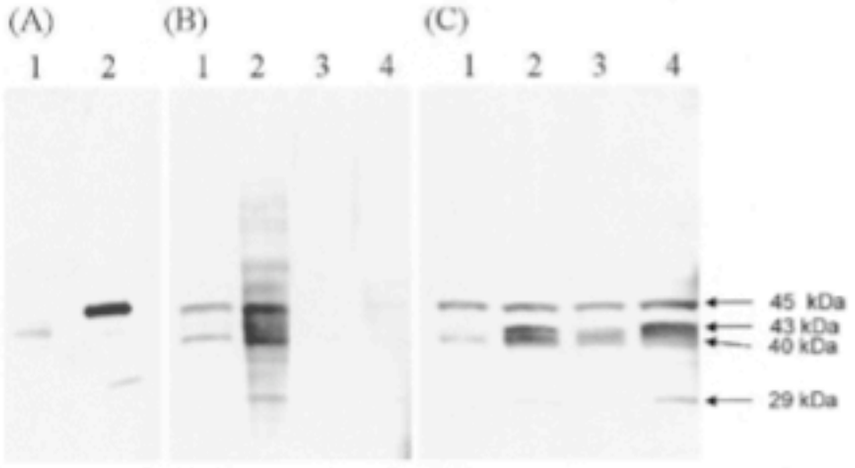

Figure 5. Western blot detection of A2BP1. (**A**) Protein extract from HTB10 cells was detected with preimmune serum (lane 1) and affinity-purified A2BP1-B antibody (lane 2). A2BP1-B antibody detected a protein of 45 kDa which was not detected by the preimmune serum. (**B**) Protein extracts from cerebral cortex (lanes 1 and 3) and cerebellum (lanes 2 and 4) were detected by A2BP1-B antibody (lanes 1 and 2) or by A2BP1-B antibody preabsorbed with peptide A2BP1-B (lanes 3 and 4). Two bands of 45 and 40 kDa were detected in both cortex and cerebellum. In addition, a faint band of 29 kDa was detected in the cerebellum (lane 2). All bands were absorbed out by incubation of A2BP1-B antibody with peptide A2BP1-B (lanes 3 and 4). (**C**) Protein extracts from a neurologically normal brain (lanes 1 and 2) and SCA2 brain (lanes 3 and 4) were detected with A2BP1-B antibody. Two major bands of 45 and 40 kDa and a fainter 29 kDa band were detected in all the samples tested: normal cortex (lane 1), normal cerebellum (lane 2), SCA2 cortex (lane 3) and SCA2 cerebellum (lane 4). An extra 43 kDa band was detected in normal cerebellum (lane 1) and SCA2 cerebellum (lane 3). No significant differences were observed between normal and SCA2 brains.

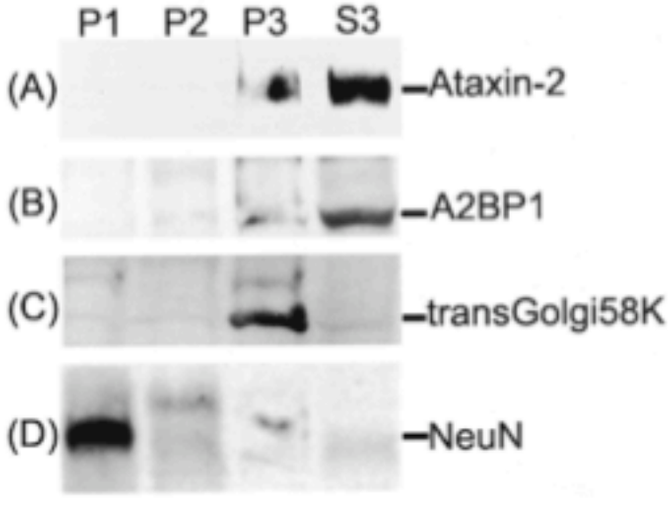

Figure 6. Western blot detection of subcellular protein fractions from human tissues. P1, nuclear fraction; P2, mitochondrial fraction; P3, ER/Golgi fraction; S3, cytosolic fraction. Fifty milligrams of protein was loaded on each lane and detected by SCA2-A antibody (**A**) or A2BP1-B antibody (**B**). The subcellular protein extracts were tested with antibody to *trans*-Golgi 58K (**C**) or NeuN protein (**D**) to confirm the efficiency of the subcellular fractionation.

HKEKDLE; peptide SCA2-B, amino acids 904–921, AAEQVRKSTLNPNAKEFN) conjugated to keyhole limpet hemocyanin. SCA2-B antibody was affinity purified by the peptide column method using antiserum 1262 as previously described (23). A rabbit anti-A2BP1 antiserum, 1734-2, was raised against peptide A2BP1-B (amino acids 177–190 of human A2BP1, TNKKTVNPYTMGWK). The fifth bleed of antiserum 1734-2 was used in co-immunoprecipitation. Antibody A2BP1-B was affinity purified with an A2BP-B peptide affinity column using antiserum 1734-2. Mouse monoclonal antibodies to γ-adaptin and *trans*-Golgi 58K was purchased from Sigma and the NeuN and 1C2 antibodies were purchased from Chemicon.

Protein extraction and western blots

Frozen brain tissues from frontal cerebrum and cerebellum were obtained from a 41-year-old SCA2 patient and a neurologically normal 32-year-old patient. Frozen tissue samples were obtained from necropsy brains within 24 h of death and stored at –70°C. Frozen tissues were resuspended in triple detergent buffer (100 mM Tris–HCl, pH 7.4, 1 mM EGTA, 1% NP-40, 0.5% SDS, 0.5% deoxycholic acid, 1 mM Pefabloc SC, 1 µg/ml pepstatin A, 2 µg/ml aprotinin and 50 µg/ml leupeptin) and homogenized using a polytron homogenizer. The protein extracts were first centrifuged at 1000 *g* (3100 r.p.m. in a JA17 rotor) for 5 min. The supernatant was recentrifuged at 105 000 *g* (54 000 r.p.m. in a TLN100 rotor) for 1 h, aliquoted and stored at –80°C. Protein concentrations were determined using the Bradford Protein Assay Kit (Bio-Rad, Hercules, CA). Prior to loading onto polyacrylamide gels, proteins were concentrated using a Microcon 10 (Amicon) concentrator or acetone precipitation. An aliquot of 100 µg of protein was loaded per lane in a precast 4–20% gradient SDS–polyacrylamide minigel (Bio-Rad) and electrophoresed at 100 V for 1–2 h. Proteins were transferred to a nitrocellulose filter (Amersham, Arlington Heights, IL). The filter was rinsed briefly with TBS (150 mM NaCl, 50 mM Tris–HCl, pH 8.0) and blocked for 1 h with 5% non-fat dried milk (Bio-Rad) for rabbit custom-made primary antibodies. The filter was then incubated with the desired dilution of test antibodies for 1 h at room temperature. The primary antibodies were detected by an ECL western blotting detection system (Amersham) using anti-rabbit IgG antibodies conjugated with horseradish peroxidase.

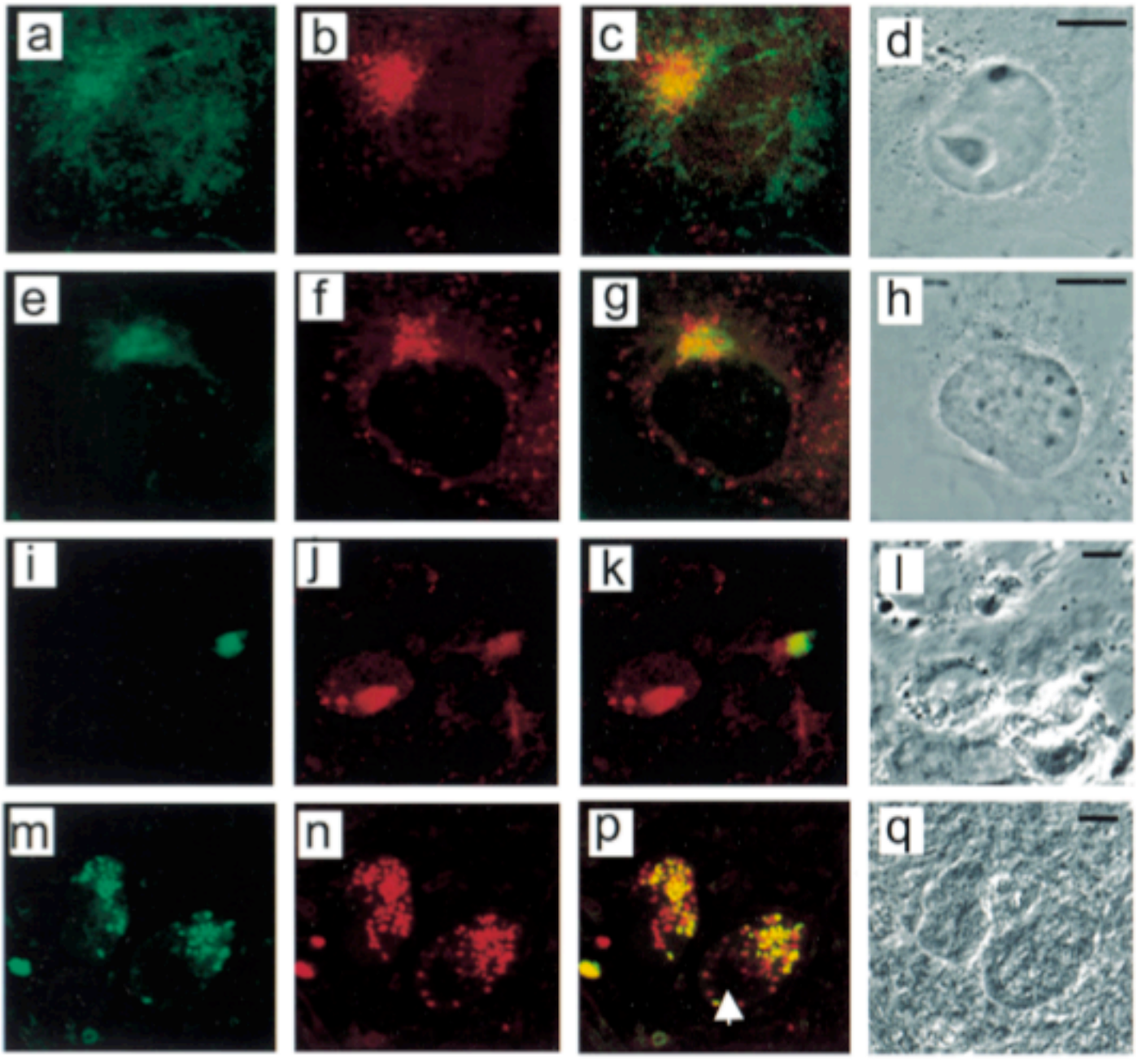

Figure 7. Co-localization of A2BP1 and ataxin-2. (a–h) Co-localization of ataxin-2, A2BP1 and γ-adaptin in COS1 cells. COS1 cells were co-labeled with the SCA2A antibody (**a**) and a mouse antibody to γ-adaptin (**b**). (**c** and **d**) Composites and phase contrast images of (a) and (b). COS1 cells co-labeled with the A2BP1-B antibody (**e**) and the γ-adaptin antibody (**f**). (**g** and **h**) Composites and phase contrast images of panels (e) and (f). (i–l) Co-localization of A2BP1 with GFP–ataxin-2(Q22) fusion protein. (i) COS1 cells transiently transfected with pEGFP-SCA2(Q22) and stained with A2BP1-B antibody (j). (**k** and l) Composites and phase contrast images of panels (i) and (j). (m–p) Co-localization of A2BP1 and mutant ataxin-2 in SCA2 brain. (**m** and **n**) Human dentate neurons from an SCA2 patient co-labeled with the A2BP1-B (m) and 1C2 (n) antibodies. (**p**) A composite of A2BP1 and 1C2 labeling showing co-localization of A2BP1 with most, but not all, 1C2-labeled structures. The white arrow in (p) indicates the nucleus of the dentate neuron. Scale ba,r 5 μm.

Immunofluorescent cytochemistry

To determine the cellular co-localization of ataxin-2 and A2BP1, COS1 cells were grown in 4-well tissue culture slides for 72 h in DMEM with 10% FBS. Transfection of pEGFP-SCA2 (22) into COS1 cells was performed using SuperFect Transfection Reagents (Qiagen, Valencia, CA). Cells were washed with DPBS three times at room temperature and incubated with 4% paraformaldehyde (Sigma, St Louis, MO) for 10 min. The fixed cells were preincubated for 30 min with 3% goat serum in DPBS. The cells were then co-stained for 1 h at room temperature with a 1:20-fold dilution of mouse monoclonal antibody to γ-adaptin and 10 μg/ml of either SCA2A or A2BPB antibody. The primary antibodies were detected with a 1:200-fold dilution of FITC-conjugated goat anti-rabbit IgG and TRITC-conjugated anti-mouse IgG (Sigma). Images were acquired using a Zeiss LSM 310 confocal microscope.

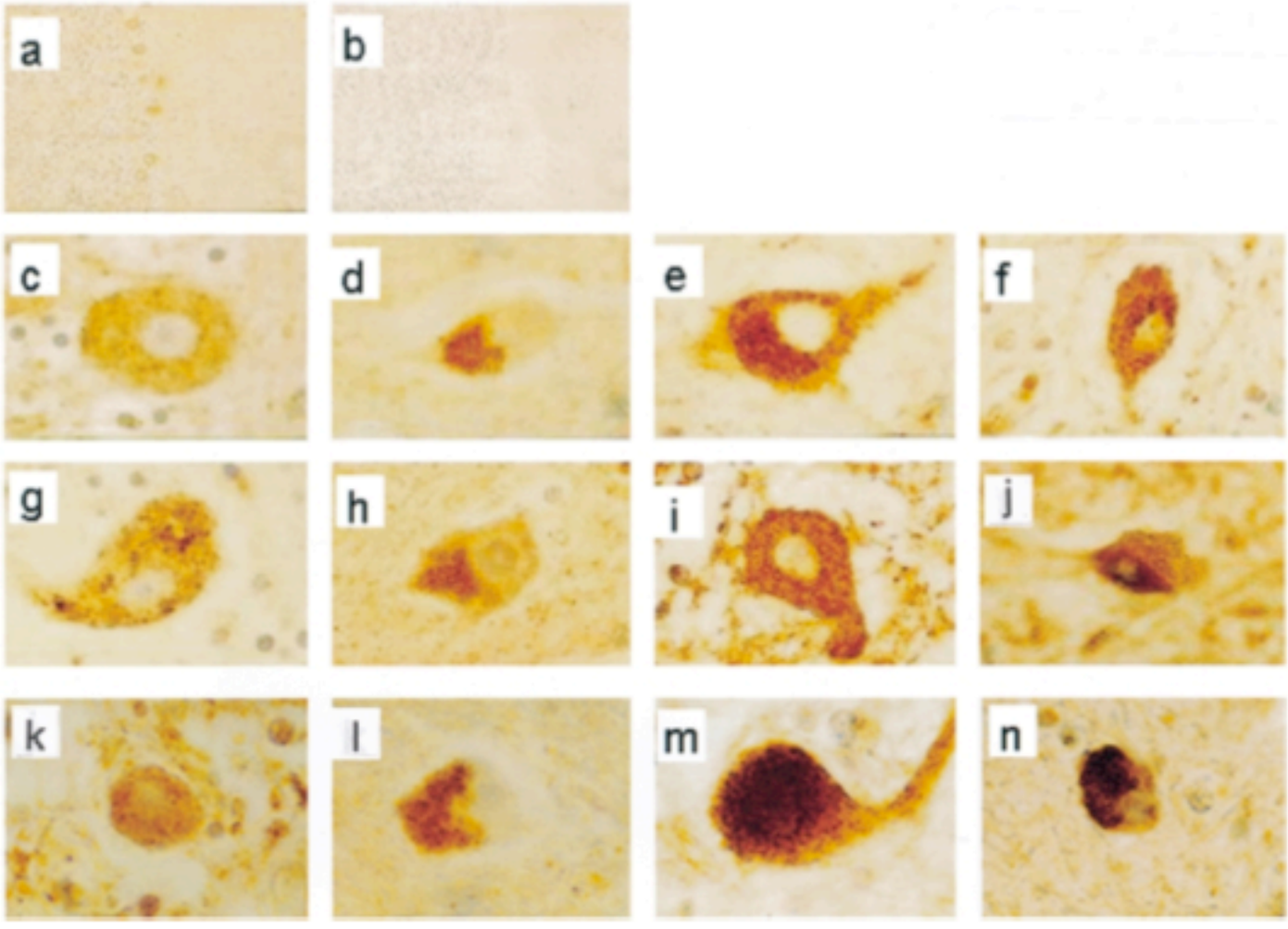

Figure 8. A2BP1 and ataxin-2 labeling in normal and SCA2 cerebellum. (**a**) Normal Purkinje cells stained with A2BP1-B antibody and (**b**) an adjacent section stained with A2BP1-B preabsorbed with A2BP1-B peptide. (**c** and **d**) Normal Purkinje cells (c) and dentate neurons (d) labeled with the A2BP1-B antibody. (**e** and **f**) Purkinje cells (e) and dentate neurons (f) from an SCA2 patient labeled with A2BP1-B antibody. (**g** and **h**) Normal Purkinje cells (g) and dentate neurons (h) labeled with the SCA2-B antibody. (**i** and **j**) Purkinje cells (i) and dentate neurons (j) from an SCA2 patient labeled with SCA2-B antibody. (**k**–**n**) A2BP1-B antibody labeling of normal (k and l) and SCA2 (m and n) cerebella from a second set of control and SCA2 brains. Magnification: (a) and (b) ×100; (c)–(n) ×500.

Co-immunoprecipitation

Human HTB10 neuroblastoma cells were grown to 80% confluency in DMEM with 10% FBS, washed in PBS and harvested in RIPA buffer (50 mM Tris–HCl, pH 7.5, 150 mM NaCl, 0.1% SDS, 0.5% deoxycholic acid, 1% Tween-20 and 0.05% NaN_3) containing 2 mg/ml aprotinin, 1 mg/ml leupeptin, 500 mg/ml Pefabloc SC and 1 mg/ml pepstatin. The lysates were precleared with rabbit serum agarose (Sigma) and then with formalin-fixed *Staphylococcus aureus* cells (Sigma) at room temperature for 1 h, respectively. The precleared lysate was incubated with anti-ataxin-2 serum (1262-1) or anti-A2BP1 serum (1734-2) at 4°C overnight. Thereafter, protein A/G resin (CytoSignal) was added to the lysate and incubated at 4°C for 1 h to recover the antigen–antibody complex. The resin was washed several times with RIPA buffer. The precipitated proteins were recovered from the resin through a spin filter column (CytoSignal) by centrifugation with 2× sample buffer (62.5 mM Tris, pH 6.8, 4% SDS, 20% glycerol, 5% β-mercaptoethanol and 0.0025% bromophenol blue) and analyzed on a western blot using SCA2-B antibody. Expression levels of endogenous A2BP1 and ataxin-2 in native HTB10 cells were confirmed by western blot analysis (data not shown).

Subcellular fractionation

HTB10 cells at 80% confluency or frozen human cerebral cortex tissues were homogenized in lysis buffer (100 mM Tris–HCl, pH 7.4, 1 mM EGTA, 0.4% sucrose, 2 mg/ml aprotinin, 0.5 mg/ml Pefabloc SC, 1.0 mg/ml pepstatin and 1.0 mg/ml leupeptin). The lysate was centrifuged at 1000 *g* for 20 min. The pellet was resuspended in lysis buffer and saved as the nuclear fraction, P1. The supernatant (S1) was further centrifuged at 10 000 *g* for 20 min. The pellet was resuspended in lysis buffer and saved as the mitochondrial fraction, P2. The supernatant (S2) was ultracentrifuged at 105 000 *g* for 1 h. The pellet was resuspended in lysis buffer and saved as the ER/Golgi fraction (P3). The supernatant (S3) was saved as the

cytosolic fraction. Protein concentrations of the fractions were determined by the Bradford assay (Bio-Rad).

Immunohistochemistry

Human brain tissues obtained at necropsy were fixed with 10% formalin within 24 h of death and embedded in paraffin. Tissues from multiple sites in the brain were taken from a 40-year-old neurologically normal male. Six micron sections were cut and mounted onto Superplus microscopic slides (Fisher Scientific, Springfield, NJ). Immunohistochemistry was performed as previously described (23). Sections were rehydrated by rinsing twice at 5 min intervals in xylene, 100% ethanol, 95% ethanol and 70% ethanol. After deparaffinization, sections were treated with a protease cocktail, blocked with avidin/biotin and 3% normal goat serum. Sections were then incubated with 20 µg/ml SCA2-B or A2BP1 antibody overnight at 4°C. Primary antibodies were detected using the rabbit Vector ABC Elite Peroxidase kit (Vector), enhanced with diaminobenzidine enhancer and visualized with diaminobenzidine (Biomeda). Sections were counterstained with aqueous hematoxylin (Xymed). Controls consisted of antibodies preabsorbed with 100 µM peptide A2BP-B and preimmune sera at comparable concentrations (1/500). All slides were processed in a single batch to minimize variability.

ACKNOWLEDGEMENTS

All human brain specimens were obtained from the Health Sciences Centre in Winnipeg, Canada (kindly provided by Dr M. DelBigio). Necropsy permission forms included a clause allowing use of tissue for research purposes. We thank Tramy Vo, Karla P. Figueroa and Alisa Schlesinger for technical assistance and Daniel R. Scoles PhD for critical comments. This work was supported by the Carmen and Louis Warschaw Endowment Fund and NIH grants RO1-NS33123 and RO1-NS37883 to S.M.P. The authors acknowledge the support of the General Clinical Research Center (M01-RR00425).

NOTE ADDED IN PROOF

Through additional database queries we recently became aware of the identity of the ataxin-2 binding protein in *C.elegans*. The *C.elegans* protein is known as fox-1.

REFERENCES

1. The Huntington's Disease Collaborative Research Group (1993) A novel gene containing a trinucleotide repeat that is expanded and unstable on Huntington's disease chromosome. *Cell*, **72**, 971–983.
2. La Spada, A.R., Wilson, E.M., Lubahn, D.B., Harding, A.E. and Fischbeck, K.H. (1991) Androgen receptor gene mutations in X-linked spinal and bulbar muscular atrophy. *Nature*, **352**, 77–79.
3. Koide, R., Ikeuchi, T., Onodera, O., Tanaka, H., Igarashi, S., Endo, K., Takahashi, H., Kondo, R., Ishikawa, A., Hayashi, T. *et al.* (1994) Unstable expansion of CAG repeat in hereditary dentatorubral-pallidoluysian atrophy (DRPLA). *Nature Genet.*, **6**, 9–13.
4. Nagafuchi, S., Yanagisawa, H., Sato, K., Shirayama, T., Ohsaki, E., Bundo, M., Takeda, Y., Todokoro, K., Kondo, I., Murayama, N. *et al.* (1994) Dentatorubral and pallidoluysian atrophy expansion of an unstable CAG trinucleotide on chromosome 12p. *Nature Genet.*, **6**, 14–18.
5. Orr, H.T., Chung, M., Banfi, S., Kwiatkowski Jr, T.J., Servado, A., Beaudet, A.L., McCall, A.E., Duvic, L.A., Ranum, L.P.W. and Zoghbi, H.Y. (1993) Expansion of an unstable trinucleotide CAG repeat in spinocerebellar ataxia type 1. *Nature Genet.*, **6**, 14–18.
6. Pulst, S.-M., Nechiporuk, A., Nechiporuk, T., Gispert, S., Chen, X.-C., Lopes-Cendes, I., Pearlman, S., Lunkes, A., de Jong, P., Rouleau, G.A. *et al.* (1996) Moderate expansion of a normally biallelic trinucleotide repeat in spinocerebellar ataxia type 2. *Nature Genet.*, **14**, 269–276.
7. Sanpei, K., Takano, H., Igarashi, S., Sato, T., Oyake, M., Sasaki, H., Wakisaka, A., Tashiro, K., Ishida, Y., Ikeuchi, T. *et al.* (1996) Identification of the spinocerebellar ataxia type 2 gene using a direct identification of repeat expansion and cloning technique, DIRECT. *Nature Genet.*, **14**, 277–284.
8. Imbert, G., Saudou, F., Yvert, G., Devys, D., Trottier, Y., Garnier, J.M., Weber, C., Mandel, J.-L., Cancel, G., Abbas, N. *et al.* (1996) Cloning of the gene for spinocerebellar ataxia 2 reveals a locus with high sensitivity to expanded CAG/glutamine repeats. *Nature Genet.*, **14**, 285–291.
9. Kawaguchi, Y., Okamoto, T., Taniwaki, M., Aizawa, M., Inoue, M., Katayama, S., Kawakami, H., Nakamura, S., Nishimura, M., Akiguchi, I. *et al.* (1994) CAG expansion in a novel gene for Machado-Joseph disease at chromosome 14q32.1. *Nature Genet.*, **8**, 221–227.
10. Zhuchenko, O., Bailey, J., Bonnen, P., Ashizawa, T., Stockton, D.W., Amos, C., Dobyns, W.B., Subramony, S.H., Zoghbi, H.Y. and Lee, C.-C. (1997) Autosomal dominant cerebellar ataxia (SCA6) associated with small polyglutamine expansions in the a1A-voltage-dependent calcium channel. *Nature Genet.*, **15**, 62–69.
11. David, G., Abbas, N., Stevanin, G., Dürr, A., Yvert, G., Cancel, G., Weber, C., Imbert, G., Saudou, F., Antoniou, E. *et al.* (1997) Cloning of the SCA7 gene reveals a highly unstable CAG repeat expansion. *Nature Genet.*, **17**, 65–70.
12. Scherzinger, E., Lurz, R., Turmaine, M., Mangiarini, L., Hollenbach, B., Hasenbank, R., Bates, G.P., Davies, S.W., Lehrach, H. and Wanker, E.E. (1997) Huntingtin-encoded polyglutamine expansions form amyloid-like protein aggregates *in vitro* and *in vivo*. *Cell*, **90**, 549–558.
13. Li, S.-H. and Li, X.-J. (1998) Aggregation of N-terminal huntingtin is dependent on the length of its glutamine repeats. *Hum. Mol. Genet.*, **7**, 777–782.
14. Cooper, J.K., Schilling, G., Peters, M.F., Herring, W.J., Sharp, A.H., Kaminsky, Z., Masone, J., Khan, F.A., Delanoy, M., Borchelt, D.R. *et al.* (1998) Truncated N-terminal fragments of huntingtin with expanded glutamine repeats form nuclear and cytoplasmic aggregates in cell culture. *Hum. Mol. Genet.*, **7**, 783–790.
15. Paulson, H.L., Perez, M.K., Trottier, Y., Trojanowski, J.Q., Subramony, S.H., Das, S.S., Vig, P., Mandel, J.-L., Fischbeck, K.H. and Pittman, R.N. (1997) Intranuclear inclusions of expanded polyglutamine protein in spinocerebellar ataxia type 3. *Neuron*, **19**, 333–344.
16. Davies, S.W., Turmaine, M., Cozens, B.A., DiFiglia, M., Sharp, A.H., Ross, C.A., Scherzinger, E., Wanker, E.E., Mangiarini, L. and Bates, G.P. (1997) Formation of neuronal intranuclear inclusions underlies the neurological dysfunction in mice transgenic for the HD mutation. *Cell*, **90**, 537–548.
17. Martindale, D., Hackam, A., Wieczorek, A., Ellerby, L., Wellington, C., McCutcheon, K., Singaraja, R., Esfarjani, P.K., Devon, R, Kim, S.U. *et al.* (1998) Length of huntingtin and its polyglutamine tract influences localization and frequency of intranuclear aggregates. *Nature Genet.*, **18**, 150–154.
18. DiFiglia, M., Sapp, E., Chase, K.O., Davies, S.W., Bates, G.P., Vonsattel, J.P. and Aronin N. (1997) Aggregaion of huntingtin in neural intranuclear inclusions and dystrophic neurites in brain. *Science*, **277**, 1990–1993.
19. Igarashi, S., Koide, R., Shimohata, T., Yamada, M., Hayashi, Y., Takano, H., Date, H., Oyake, M., Sato, T., Sato, A. *et al.* (1998) Suppression of aggregate formation and apoptosis by transglutaminase inhibitors in cells expressing truncated DRPLA protein with an expanded polyglutamine stretch. *Nature Genet.*, **18**, 111–117.
20. Holmberg, M., Duyckaerts, C., Dürr, A., Cancel, G., Gourfinkel-An, I., Damier, P., Faucheux, B., Trottier, Y., Hirsch, E.C., Agid, Y. and Brice, A. (1998) Spinocerebellar ataxia type 7 (SCA7): a neurodegenerative disorder with neuronal intranuclear inclusions. *Hum. Mol. Genet.*, **7**, 913–918.
21. Klement, I.A., Skinner, P.J., Kaytor, M.D., Yi, H., Hersch, S.M., Clark, H.B., Zoghbi, H.Y. and Orr, H.T. (1998) Ataxin-1 nuclear localization and aggregation: role in polyglutamine-induced disease in SCA1 transgenic mice. *Cell*, **95**, 41–53.
22. Saudou, F., Finkbeiner, S., Devys, D. and Greenberg M.E. (1998) Huntingtin acts in the nucleus to induce apoptosis but death does not correlate with the formation of intranuclear inclusions. *Cell*, **95**, 55–66.

23. Huynh, D.P., Del Bigio, M.R., Ho, D.H. and Pulst, S.-M. (1999) Expression of ataxin 2 in brains from normal individuals and patients with Alzheimer's disease and spinocerebellar ataxia 2 (SCA2). *Ann. Neurol.*, **45**, 232–241.
24. Rotonda, J., Nocholson, D.W., Fazil, K.M., Gallant, M., Gareau, Y., Labelle, M., Peterson, E.P., Rasper, D.M., Ruel, R., Vaillancourt, J.P. *et al.* (1996) The three-dimenstional structure of apopain/CPP32, a key mediator of apoptosis. *Nature Struct. Biol.*, **3**, 619–627.
25. Neuwald, A.E. and Koonin, E.V. (1998) Ataxin-2, global regulators of bacterial gene expression and splicesomal snRNP proteins share a conserved domain. *J. Mol. Med.*, **76**, 3–5.
26. Bannykh, S.I., Nishimura, N. and Balch, W.E. (1998) Getting into the Golgi. *Trends Cell Biol.*, **8**, 21–25.
27. Pulst, S.-M. (1998) Spinocerebellar ataxia type 2. In *Genetic Instabilities and Hereditary Neurological Diseases*. Academic Press, New York, NY, Ch. 20, pp. 265–271.
28. Sittler, A., Walter, S., Wedemeyer, N., Hasenbank, R., Scherzinger, E., Eickhoff, H., Bates, G.P., Lehrach, H. and Wanker, E.E. (1998) SH3GL3 associates with the huntingtin exon 1 protein and promotes the formation of polyGln-containing protein aggregates. *Mol. Cell*, **2**, 427–436.
29. Wanker, E., Rovira, C., Scherzinger, E., Hasenbank, R., Walter, S., Tait, D., Colicelli, J. and Lehrach, H. (1997) HIP-1: a huntingtin interacting protein isolated by the yeast two-hybrid system. *Hum. Mol. Genet.*, **6**, 487–495.
30. Kalchman, M., Koide, H.B., McCutcheon, K., Graham, R.K., Nichol, K., Nishiyama, K., Kazemi-Esfarjani, P., Lynn, F.C., Wellington, C., Metzler, M. *et al.* (1997) HIP1, a human homologue of S. cerevisiae Sla2p, interacts with membrane-associated huntingtin in the brain. *Nature Genet.*, **16**, 44–53.
31. Kalchman, M.A., Graham, R.K., Xia, G., Koide, H.B., Hodgson, J.G., Graham, K.C., Goldberg, Y.P., Gietz, R.D., Pickart, C.M. and Hayden, M.R. (1996) Huntingtin is ubiquitinated and interacts with a specific ubiquitin-conjugating enzyme. *J. Biol. Chem.*, **271**, 19385–19394.
32. Boutell, J.M., Wood, J.D., Harper, P.S. and Jones, A.L. (1998) Huntingtin interacts with cystathionine β-synthase. *Hum. Mol. Genet.*, **7**, 371–378.
33. Li, X.-J., Li, S.-H., Sharp, A.H., Nucifora, F.C., Schilling, G., Lanahan, A., Worley, P., Snyder, S.H. and Ross, C.A. (1995) A huntingtin-associated protein enriched in brain with implications for pathology. *Nature*, **378**, 398–402.
34. Faber, P.W., Barnes, G.T., Srinidhi, J., Chen, J., Gusella, J.F. and MacDonald, M.E. (1998) Huntingtin interacts with a family of WW domain proteins. *Hum. Mol. Genet.*, **7**, 1463–1474.
35. Wood, J.D., Yuan, J., Margolis, R.L., Colomer, V., Duan, K., Kushi, J., Kaminsky, Z., Kleiderlein, J.J., Sharp, A.H. and Ross, C.A. (1998) Atrophin-1, the DRPLA gene product, interacts with two families of WW domain-containing proteins. *Mol. Cell Neurosci.*, **11**, 149–160.
36. Matilla, A., Koshy B.T., Cummings, C.J., Isobe, T., Orr, H.T. and Zoghbi, H.Y. (1997) The cerebellar leucine-rich acidic nuclear protein interacts with ataxin-1. *Nature*, **389**, 974–978.
37. Burd, C.G. and Dreyfuss, G. (1994) Conserved structures and diversity of functions of RNA-binding proteins. *Science*, **265**, 615–621.
38. Miller, J.H. (1972) *Experiments in Molecular Genetics*. Cold Spring Harbor Laboratory Press, Cold Spring Harbor, NY.